

Channel Sounding for High-Speed Railway Communication Systems

Journal:	<i>IEEE Communications Magazine</i>
Manuscript ID:	COMMAG-15-00230
Topic or Series:	October 2015/Future Railway Communications
Date Submitted by the Author:	31-Mar-2015
Complete List of Authors:	Zhou, Tao; Institute of Broadband Wireless Mobile Communications, Beijing Jiaotong University Tao, Cheng; Institute of Broadband Wireless Mobile Communications, Beijing Jiaotong University Salous, Sana; School of Engineering and Computing Sciences, Durham University Liu, Liu; Institute of Broadband Wireless Mobile Communications, Beijing Jiaotong University Tan, Zhenhui; Institute of Broadband Wireless Mobile Communications, Beijing Jiaotong University
Key Words:	Channel sounding, High-speed railway, Railway communication system, Channel measurement

SCHOLARONE™
Manuscripts

Only

Channel Sounding for High-Speed Railway Communication Systems

Tao Zhou¹, Cheng Tao¹, Sana Salous², Liu Liu¹, Zhenhui Tan¹

¹Institute of Broadband Wireless Mobile Communications, Beijing Jiaotong University, Beijing 100044, P.R.China

²School of Engineering and Computing Sciences, Durham University, Durham DH1 3LE, UK

Email: taozhou.china@gmail.com, chtao@bjtu.edu.cn, sana.salous@durham.ac.uk, {liuliu, zhhtan}@bjtu.edu.cn

Abstract

High-speed railway (HSR) communications have recently attracted much attention due to some specific railway needs, such as passenger experience services, business process support services, and operational data and voice services. The HSR radio channel, as a basis for the design of HSR communication systems and the evaluation of HSR communication technologies, has not yet been sufficiently investigated. This article focuses on radio channel sounding techniques for future HSR communication systems. Emphasis is placed on the fundamental features for measuring the HSR channel and a review of the state-of-the-art in HSR channel measurements is given. We also propose a novel long term evolution (LTE) based HSR channel sounding scheme and present results from our own measurement campaigns.

Introduction

The rapid development of high-speed railway (HSR) transport has led to a growth in demand for broadband wireless communication services both from train operators and from passengers. In Europe and China, train operators employ the global system for mobile communications for railway (GSM-R), a narrow-band communication system, to maintain reliable train to ground communication. To guarantee train operational safety, in addition to standard train control services involving dispatching, shunting and maintenance, broadband services such as onboard video surveillance and track monitoring are becoming more and more important. These services, however, are beyond the reach of GSM-R. Besides the security requirements, it is necessary to enhance the comfort and satisfaction of passengers who expect to enjoy high-quality in-journey services, e. g., mobile services, online TV and Internet access. With the understanding of rail operational demands as well as rail passenger communications needs, the next-generation HSR communication system [1] and the novel HSR wireless network architecture [2] need to be developed to

1
2
3 provide a variety of services for safety and infotainment.
4

5 An example of future HSR communication systems is illustrated in Fig. 1. The potential key
6 communication technologies in this system involve cell combination [3], mobile relay [4], multiple-input
7 multiple-output (MIMO), and coordinated multipoint transmission (CoMP) [5]. In the following we briefly
8 introduce typical features of these techniques.
9
10

- 11 • **Cell Combination** - The high mobility of the receiver yields frequent handovers in communication
12 networks, e. g., when a train is running at 300 km/h and inter-site distance along the rail is 1.2 km,
13 handovers occur every 7 seconds. Such frequent handovers lead to a large amount of signaling or
14 even to a signaling storm. Cell combination is used to reduce the handover frequency in high speed
15 scenarios, which combines several base stations (BSs) into a big virtual cell. However, in this
16 architecture the receiver could suffer from interference among neighboring BSs.
17
- 18 • **Mobile Relay** - Mobile relay is employed for multi-hop coverage from BS to mobile relay station
19 (MRS), and to user equipment (UE) or other onboard devices, such as camera, TV, and access point
20 (AP). The train access unit (TAU), as a MRS, which can support one or many technology types,
21 connects to the access network using antennas mounted on the outside of the train car. In addition,
22 in-train networks can be organized to support various communication services. The mobile relay is
23 expected to avoid the penetration loss from the train body, but the train roof could cause distorted
24 antenna radiation, affecting the received power.
25
- 26 • **MIMO** - MIMO is an important technology that can effectively exploit the spatial domain of mobile
27 fading channels to enhance the capacity of wireless communication systems. Due to the special
28 features of the HSR channel which is dominated by the line of sight (LOS) component, HSR
29 scenarios are not favorable for the application of MIMO technology. However, there is sufficient
30 space on top of the train for distributed MRS antennas which can be deployed at appropriate spacing
31 to improve MIMO performance.
32
- 33 • **CoMP** - CoMP is an emerging innovative technology for improving the transmission efficiency
34 since it can transform the interference from the cooperative BSs into useful signals by coordinated
35 transmission and reception. Applying CoMP in HSR communication systems is a good idea which
36 not only mitigates the interference caused by the cell combination but also exploits the diversity gain
37 to enhance capacity. The BSs in the combined cell should be connected to a backhaul network which
38 is used to exchange the information involving data, control information, and channel state
39
40
41
42
43
44
45
46
47
48
49
50
51
52
53
54
55
56
57
58
59
60

information (CSI).

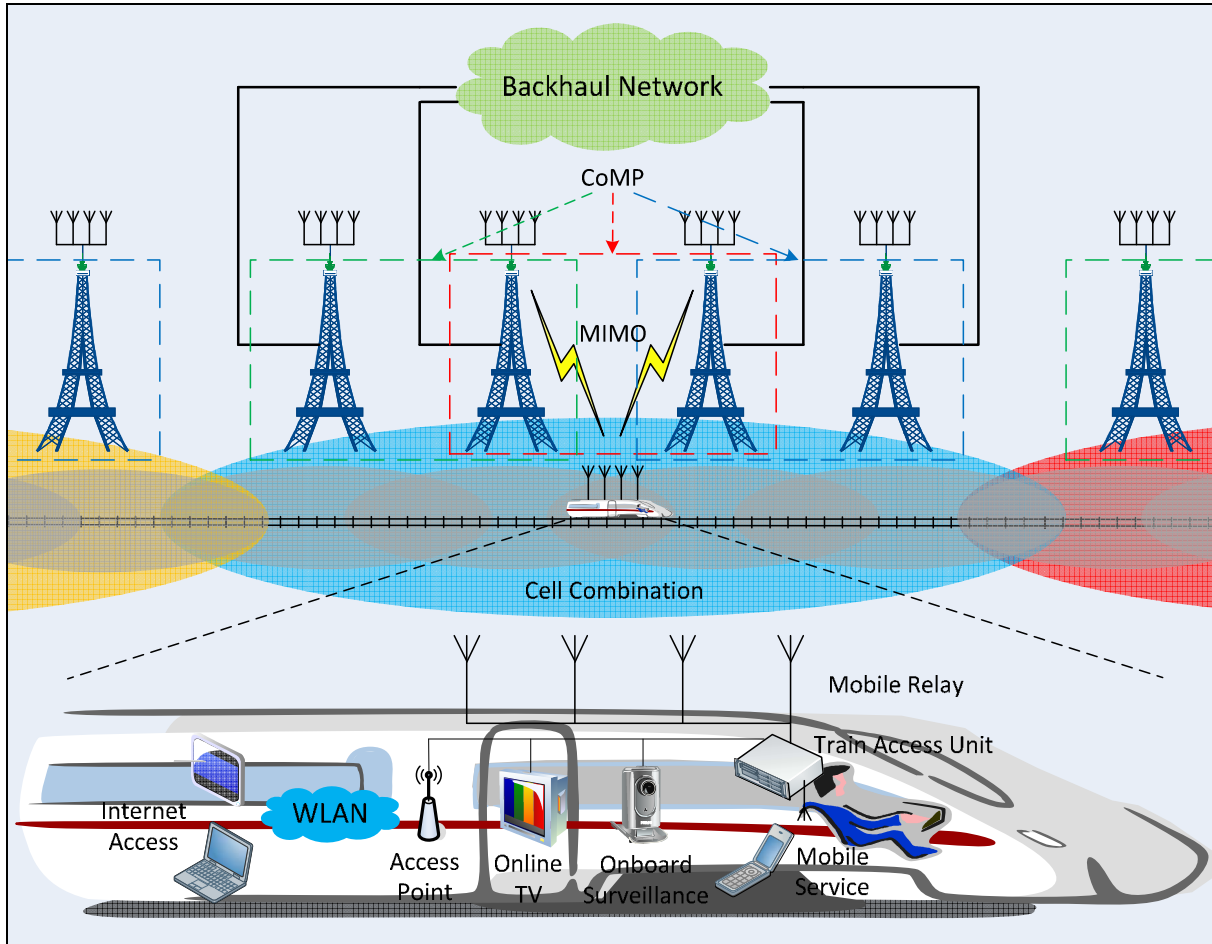


Figure 1. Future HSR communication system

Since the radio channel determines the performance of wireless communication systems, detailed knowledge and accurate characterization of its parameters in realistic HSR propagation scenarios is crucial. The majority of radio channel models used for system simulation are based on extensive channel measurement data. Therefore, channel sounding is a precondition for the design of HSR communication systems and the evaluation of HSR communication technologies. Though measurement campaigns on HSR are expensive, time-consuming, and difficult to carry out, a few HSR channel measurements have been conducted such as those reported in [6-8] using radio channel sounders or railway network based measurements [9-10]. As future HSR communication systems will apply MIMO and CoMP, channel measurements should consider the correlation properties of the individual links and multiple links which significantly affect the performance of MIMO and CoMP. In addition, the impact of using cell combination and mobile relay also needs to be evaluated according to channel measurements in real-world HSR wireless networks. Until now, to the best of

our knowledge, there was no appropriate HSR channel sounding method that can be used to carry out related channel measurements addressing these issues.

Motivated by this observation, this article aims to describe how to measure the HSR channel comprehensively, reliably, and efficiently. We first give an overview of HSR channel sounding techniques and then propose a novel long term evolution (LTE) based channel sounding scheme to meet the requirements and challenges in HSR channel measurements. Lastly, we provide our latest field measurement results based on the proposed scheme.

HSR Channel Sounding

In radio channel measurements, a known signal that repeats at a rate twice the highest expected Doppler shift is transmitted and the received signal is analyzed to evaluate the effects of the channel on its transmission. More specifically, in channel sounding we observe how many echoes of the signal are received and their amplitude and phase variations along the travel route. The radio channel is measured using a channel sounder that detects the electromagnetic wave transmitted via a particular communication channel to determine the statistics of either the channel impulse response (CIR) or channel frequency response (CFR). Classical channel sounding techniques can be loosely classified into two categories: narrowband or wideband. Using a continuous waveform (CW) to excite the channel is the most common narrowband channel sounding technique which only provides signal fading characteristics but does not provide information regarding the multipath components. These can be resolved using wideband techniques which involve periodic pulse sounding, and pulse compression waveforms that avoid the need for high peak transmitted power and provide processing gain. The two commonly used techniques are either coded sequence transmission or chirp sounding [11]. Another technique uses an orthogonal frequency division multiplexing (OFDM) signal to probe the channel [12]. In general, the choice of the particular waveform or technique depends on the channel sounding requirements.

Requirements in HSR Channel Measurements

The main channel measurement requirements are determined by the time delay resolution, which sets the transmitted bandwidth and the maximum expected Doppler shift which determines the waveform repetition frequency (WRF) [11]. The time delay resolution indicates the smallest difference in time delay between

1
2
3
4
5
6
7
8
9
10
11
12
13
14
15
16
17
18
19
20
21
22
23
24
25
26
27
28
29
30
31
32
33
34
35
36
37
38
39
40
41
42
43
44
45
46
47
48
49
50
51
52
53
54
55
56
57
58
59
60

resolvable multipath components, which is inversely proportional to the bandwidth of the system. In [1], the bandwidth of future HSR communication systems is recommended to be higher than 10 MHz. Thus, the minimum time delay resolution should be 100 ns for the HSR channel measurement, corresponding to a distinguishable 30 m difference in propagation distance. The WRF depends on the carrier frequency and the vehicular speed, which is at least twice the maximum expected Doppler shift. In [1], it is suggested that for HSR dedicated communications, the high priority service is working in the 800-MHz frequency band, and the low priority service is working in the 1800-MHz frequency band. At 1.8 GHz operating frequency and for measurements in HSR scenarios, the maximum expected Doppler shift can be accommodated within 600 Hz (maximum vehicular speeds of 360 km/h), and thus the WRF should exceed 1.2 kHz. The WRF also determines the maximum time delay window that refers to the overall time delay spread of a multipath and the farthest distance that can be measured. The time delay window, however, has to be in excess of the extent of multipath to allow for travel distances away from the transmitter. For instance, when the multipath components are assumed to extend over 1 μ s and the distance of two BSs in HSR communication systems is 1.2 km which corresponds to 4 μ s, the time delay window has to be in excess of 5 μ s to ensure that the movement of the multipath components is still within the observable window.

As for MIMO measurements, these requirements are essentially the same with the added requirement of multiple transmissions and multiple receptions. MIMO channel sounding can be achieved in three possible architectures. The most popular one is a full sequential architecture using time division multiplexing (TDM) mode with switching between antennas at the transmitter and at the receiver. To enable Doppler measurement the scanning of all antennas should be completed within the coherent time of the channel. For the 8 by 8 HSR MIMO channel system, the required WRF should be as high as 76.8 kHz. In contrast, a full parallel architecture employing a number of orthogonal techniques, such as code division multiplexing (CDM) and frequency division multiplexing (FDM), transmits and receives simultaneously from all antennas, which only requires the same WRF as single antenna systems. An alternative to these two architectures is a semi-sequential architecture where the transmitter is switched between the different antennas with a number of parallel receiver channels [11]. For the example of eight antennas, the needed WRF corresponds to 9.6 kHz.

Challenges in HSR Channel Measurements

While current channel sounding techniques have been quite mature and extensive measurement

1
2
3 campaigns have been reported for terrestrial cellular communication systems, there are still some challenges
4
5 in HSR channel measurements that should be addressed.
6

7 The first challenge is how to employ the commonly used channel sounding techniques in HSR
8 environments. Generally, to guarantee the security of train control network, the wireless frequency bands are
9 under surveillance by the railway administration. In addition to the existing network signals, such as GSM-R,
10 wideband code division multiple access (WCDMA), LTE, etc., any other wireless test signals are prohibited
11 from transmission along the rail. Since all conventional channel sounding techniques need to transmit a
12 particular waveform, it is difficult to directly apply these methods in HSR channel measurements.
13
14
15
16
17

18 Another challenge is how to measure MIMO and CoMP channels. The requirement of WRF in HSR
19 scenarios makes HSR MIMO channel measurement very challenging. Most of the MIMO channel sounders
20 with the full sequential architecture cannot meet such a high requirement. Although the WRF can be decreased
21 by reducing the number of transmit or receive antennas, this would degrade the angular measurement
22 capability. To enable the CoMP channel measurement, there exists a kind of static multi-link measurement
23 where single-link measurements are used to form a static multi-link scenario (see, e. g., [13]). However, such
24 an approach is not valid if parts of the channel changes between measurements at different locations. Thus,
25 multi-link channel measurements should be carefully designed and conducted using advanced channel
26 sounding equipment and techniques that can record the observations of two or more channels simultaneously.
27
28
29
30
31
32
33
34

35 The final important issue to address is the measurement efficiency which is extremely low when the
36 commonly used channel sounders are employed. For instance, if the train travels at a speed of 360 km/h and
37 the coverage radius of a channel sounder is 1 km, the recording time of the sounder is approximately 20 s. The
38 obtained experimental data in this short period may not be adequate to extract the statistical properties of the
39 HSR channel. In addition, one HSR line could cover a wide variety of scenarios, such as urban, suburban,
40 rural, hilly, as well as some special scenarios like cutting, viaduct, tunnel, station, etc. Measuring all these
41 scenarios is meaningful to establish a complete and accurate HSR channel model. However, it is extremely
42 challenging when using universal channel sounders with low measurement efficiency to achieve this task.
43
44
45
46
47
48
49
50

51 **Recent Advances in HSR Channel Measurements**

52 In this section, we will briefly review some recent typical HSR radio channel measurement campaigns,
53
54
55 which can be simply classified into two categories, as follows:
56
57
58
59
60

- **Channel sounder based measurements** - Until now, there are only several measurement campaigns taken under high mobility conditions, using standard commercial multidimensional channel sounders with full sequential architectures, e. g., RUSK and Propsound. One of the first reported HSR measurements employed the RUSK sounder to measure the single-input multiple-output (SIMO) mobile relay channel in Germany [6]. The used waveform called multi-carrier spread spectrum signal (MCSSS) is a kind of OFDM signal, which concentrates the energy in the band of interest. Propsound HSR channel measurements in rural and hilly scenarios in Taiwan were reported in [7]. The direct link from the BS to the UE was considered to measure the SIMO and the multiple-input single-output (MISO) channel. Further, single-input single-output (SISO) mobile relay channel measurements using Propsound were carried out in viaduct scenarios on HSR in China [8]. However, there are still no reported MIMO channel measurements in a specific HSR scenario utilizing the standard commercial channel sounders.
- **Railway network based measurements** - Due to the restrictions imposed by using traditional channel sounders on HSR, since 2011 some researchers resorted to the railway network based channel sounding method. The basic idea of the method is to exploit the sounding ability of the signal transmitted from the railway network to enable continuous measurements along the whole rail. Obvious advantages of this method are the high measurement efficiency and low measurement limitation. A series of GSM-R channel measurements were conducted in viaduct scenarios on HSR in China [9]. For channel characterization purposes, the GSM-R signal is regarded as a narrowband CW signal and hence not suitable for wideband measurements. To enable the wideband channel characterization, the common pilot channel (CPICH) signal in the dedicated WCDMA network was collected and analyzed to extract the multipath properties [10]. The CPICH signal is related to a cell-specific scrambling Gold code. Unfortunately, the measurement bandwidth of this method does not meet the requirements of time delay resolution for the HSR channel, and it lacks the spatial sounding ability.

LTE-Based HSR Channel Sounding Scheme

Existing HSR channel measurement data are insufficient for the design of future HSR communication systems. It is necessary to carry out more measurements for further HSR channel characterization. Reported

measurement campaigns, do not provide a suitable approach with the potential of enabling comprehensive and efficient HSR channel sounding. Inspired by [9-10], we have investigated a novel HSR channel sounding scheme which employs LTE railway networks to implement the excitation of the time-frequency-space HSR channel [14], as shown in Fig. 2. In the following we briefly describe this scheme from three aspects involving LTE channel sounding system, LTE signal, and LTE sounder.

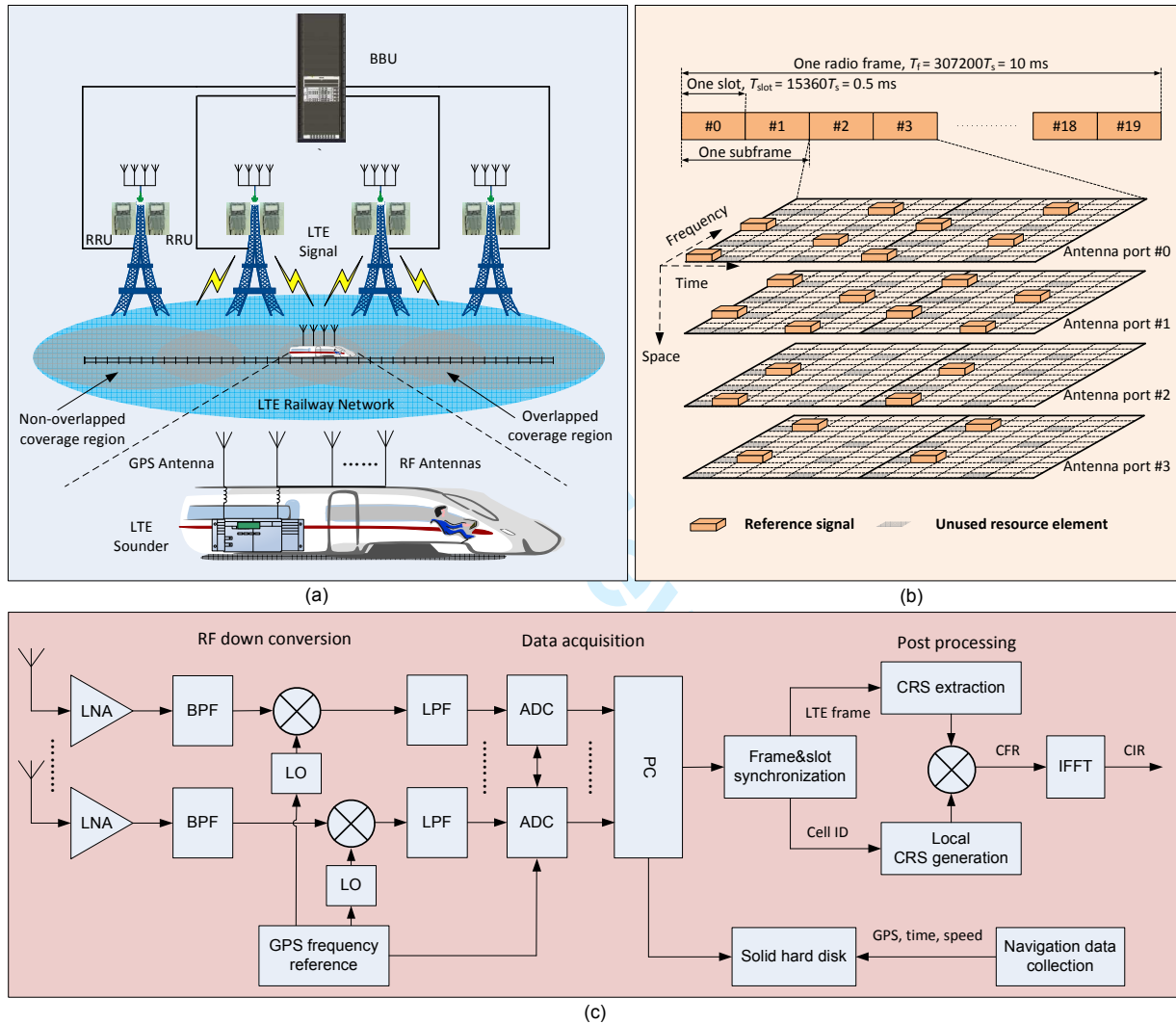


Figure 2. LTE-based HSR channel sounding scheme. (a) LTE channel sounding system. (b) Time-frequency-space FDD LTE frame structure. (c) Block diagram of LTE sounder.

LTE Channel Sounding System

LTE aims at supporting a wide variety of scenarios involving indoor, urban, suburban and rural areas covering both low and high mobility conditions. In recent years, there have been large-scale deployments of

1
2
3 LTE networks all over the world. In particular, the LTE railway network has almost covered all HSRs in China,
4 for a total of 15,000 km by 2014, and as HSRs continue to grow, LTE railway networks that grow with them
5 will exceed 30,000 km in 2020 [3]. The railway network is totally different from the conventional cellular
6 network, which adopts a kind of narrow strip coverage mode and a building baseband unit (BBU) plus remote
7 radio unit (RRU) structure. One BS site has two RRUs applying directional antennas to transmit radio
8 frequency (RF) signals in opposite directions along the track. Cell combination is employed in this network
9 where the RRUs in one cell are connected together via optical fiber and then to a BBU that is in charge of RF
10 signal processing. The entire network can be classified into two categories: non-overlapped coverage region
11 and overlapped coverage region. In the non-overlapped coverage area, only one signal is received from one
12 BS. In the overlapped area, the two same signals from neighboring BSs could arrive at the receiver
13 simultaneously, but they can be distinguished in the delay domain due to the different propagation delays. Fig.
14 2(a) illustrates an example of the LTE channel sounding system composed of the LTE railway network and the
15 LTE sounder.
16
17
18
19
20
21
22
23
24
25
26
27
28
29

30 LTE Signal

31
32
33 LTE supporting both frequency division duplexing (FDD) and time division duplexing (TDD) modes
34 adopts OFDM and MIMO technologies. Typical deployed carrier frequencies are in the range of 400 MHz to 4
35 GHz, with scalable carrier bandwidths from 1.4 MHz to 20 MHz. The time-frequency-space FDD LTE frame
36 structure is shown in Fig. 2(b). One radio frame of 10 ms is subdivided into ten 1 ms subframes, each of
37 which is split into two 0.5 ms slots. In the case of the normal cyclic prefix (CP), one slot comprises seven
38 OFDM symbols and the spacing of subcarriers in one OFDM symbol is 15 kHz. In [14], it has been shown
39 that the cell-specific reference signals (CRSs) play a key role in LTE-based channel sounding, which
40 completely determine the measurement capability. The CRSs are embedded in the LTE time-frequency-space
41 frame structure with a diamond shape. In the time direction, the maximum repetition period of the CRSs is 0.5
42 ms, corresponding to 2 kHz WRF. In the frequency direction, there is one CRS every six subcarriers with a
43 spacing of 90 kHz on each OFDM symbol. This spacing allows the maximum time delay window of 11 μ s. In
44 the case of 20 MHz LTE, the total number of CRSs on each OFDM symbol is 200, which corresponds to 18
45 MHz measurement bandwidth and 56 ns time delay resolution. In the space direction, there are 4 antenna ports
46 carrying the orthogonal CRSs. This implies the full parallel architecture with maximum 4 antennas can be
47
48
49
50
51
52
53
54
55
56
57
58
59
60

1
2
3 used at the transmitter in the proposed LTE channel sounding system. From the above analysis, we can
4 confirm that the LTE signal is able to meet the HSR channel sounding requirements outlined in the previous
5 section.
6
7
8
9

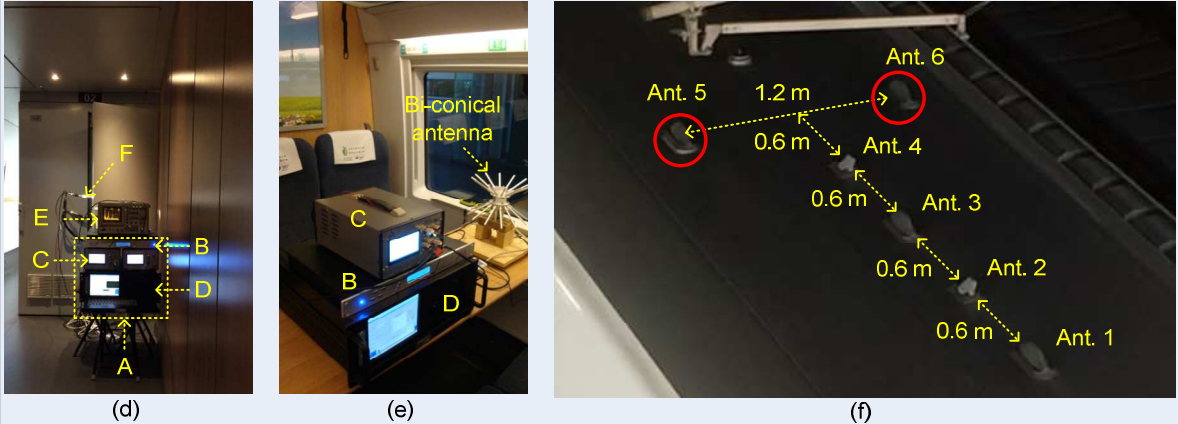
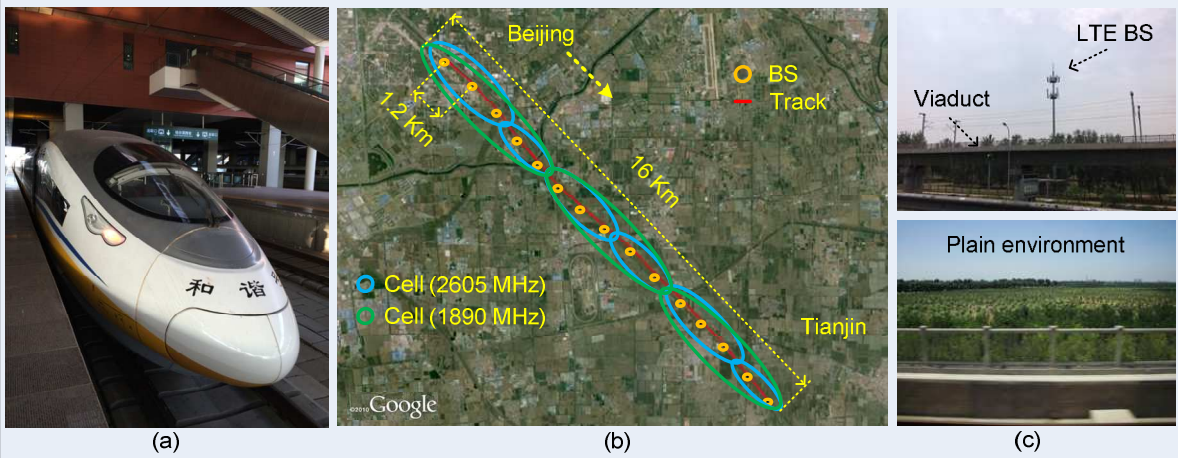
10 **LTE Sounder**

11
12
13
14 The LTE sounder is used to collect the channel data in the whole LTE railway network. Different from
15 the conventional channel sounders, the LTE sounder has only a receiver as shown in Fig. 2(c). The LTE
16 sounder with basic functions, such as RF down conversion and data acquisition, employs the same full parallel
17 architecture as the transmitter. In particular, GPS frequency reference is used to enable the frequency
18 consistency between the network and the LTE sounder. Also, baseband data and navigation data are stored
19 together in a solid state disk (SSD) for post processing. Frame and slot synchronization should be
20 implemented to acquire LTE frames and determine the cell identity (ID) for extracting the received CRS and
21 generating the local CRS, respectively. Since the CRS is OFDM modulated, frequency domain correlation [12]
22 is used to estimate the CFR which can be subsequently transformed to the CIR by inverse fast Fourier
23 transform (IFFT) operation. Reference [14] has presented simulation results to confirm the accuracy of the
24 obtained CIR.
25
26
27
28
29
30
31
32
33
34
35

36 **LTE-Based HSR Channel Sounding Results**

37
38
39 Based on the LTE railway network on Beijing to Tianjin HSR in China, we carried out LTE-based HSR
40 channel measurements on a high-speed test train, as shown in Fig. 3. Two types of scenarios, direct coverage
41 (DC) and relay coverage (RC), are considered in our measurements. We used two networks: the 2605 MHz
42 network with 6 cells was chosen for SISO DC measurements, whereas the 1890 MHz network with 3 bigger
43 cells was employed for 2×2 MIMO RC measurements. The measured environment is a typical plain viaduct,
44 as shown in Fig. 3(c). The BS is less than 20 m away from the viaduct and the BS antenna is generally 10 m,
45 20 m or 35 m higher than the rail. The measurement equipment, train-mounted antenna structure, and detailed
46 measurement parameters are illustrated in Fig. 3(d-g). In the following we present the measurement results
47 from cell combination, mobile relay, MIMO and CoMP perspectives.
48
49
50
51
52
53
54
55
56
57
58
59
60

1
2
3
4
5
6
7
8
9
10
11
12
13
14
15
16
17
18
19
20
21
22
23
24
25
26
27
28
29
30
31
32
33
34
35
36
37
38
39
40
41
42
43
44
45
46
47
48
49
50
51
52
53
54
55
56
57
58
59
60



Parameter	Value	
Transmitter		
Measurement scenario	Direct coverage	Relay coverage
Measurement frequency	2605 MHz	1890 MHz
Measurement bandwidth	18 MHz	18 MHz
CRS Power	12.2 dBm	12.2 dBm
Antenna type	$\pm 45^\circ$ cross-polarized directional	$\pm 45^\circ$ cross-polarized directional
Antenna gain	18.6 dBi	17.4 dBi
Horizontal beamwidth	60°	67°
Vertical beamwidth	4.9°	6.6°
Electric tilted angle	3°	3°
Receiver		
Antenna type	Bi-conical	HUBER+SUHNER
Antenna gain	0 dBi	8.5 dBi
Antenna number	1	2
Antenna spacing	/	1.2 m (7.6 wavelengths)
Train velocity	285 km/h	285 km/h

(g)

1
2
3 Figure 3. LTE-based channel measurements on Beijing to Tianjin HSR in China. (a) High-speed test train. (b) LTE
4 railway network structure. (c) Measurement environment. (d) Measurement equipment for the RC scenario. A: LTE
5 sounder; B: GPS frequency reference; C: RF unit; D: data acquisition card, SSD and PC; E: spectrum analyzer; F:
6 train-mounted antenna ports. (e) Measurement equipment for the DC scenario. (f) Train-mounted antenna structure. The
7 antennas 5 and 6 marked by red circles are used for the MIMO channel measurement. Antenna 1 is used to receive the
8 GPS signal. Antenna 3 is connected to the spectrum analyzer to monitor the signal state. The specific GSM-R antennas 2
9 and 4 are unused. (g) Measurement parameters.
10
11
12

13 Cell Combination Measurement Results

14
15
16
17 Fig. 4 shows results of the cell combination measurement in the RC scenario, focusing on power delay
18 profile (PDP) and Doppler power spectral density (DPSD). In Fig. 4(a), the time-variant PDP during the first
19 35 s period in a certain cell is plotted. Two obvious PDP transitions regarding BS1 and BS2 whose positions
20 are identified by the white circles are highlighted. When the train enters into the non-overlapping area, we
21 define a single-link region where one propagation link between BS1 and the train, indicated by PDP (i),
22 almost occupies the whole time delay window. However, once the train moves into the overlapping area
23 between BS1 and BS2, another propagation link between BS2 and the train, denoted by PDP (ii), appears in
24 the time delay window as well. We regard this area as a multi-link region where the time delay window covers
25 two links simultaneously. In the multi-link region, the time delay window can be divided into two parts: one is
26 for PDP (i) and another is for PDP (ii), as shown in Fig. 4(b). As the train is moving away from BS1, the delay
27 difference $\Delta\tau$ between PDP (i) and PDP (ii) is gradually shortening. If the train travels at the crossing point
28 marked with a red circle in Fig. 3(a), the PDP (i) and PDP (ii) would be indistinguishable. Since $\Delta\tau$
29 determines the time delay window of PDP (i), a threshold for $\Delta\tau$ should be set to enable the coverage of
30 most multipath components. Fig. 4(c) plots the corresponding time-variant DPSD result. When the train
31 passes through the coverage of BS1 and BS2, two typical Doppler transitions from the maximum positive
32 frequency to the minimum negative frequency are observed and marked as DPSD (i) and DPSD (ii). In the
33 single-link region only DPSD (i) exists, while in the multi-link area DPSD (i) and DPSD (ii) appear at the
34 same time, as shown in Fig. 4 (d). The two DPSDs have the same maximum Doppler shift but opposite angles
35 of arrival.
36
37
38
39
40
41
42
43
44
45
46
47
48
49
50
51

52 The results in Fig. 4 confirm that the cell combination causes a sort of artificial multipath interference
53 and Doppler interference. From the engineering perspective, to cope with such interference, the BSs are
54 normally deployed with a reasonable spacing which should ensure that the maximum propagation delay
55
56
57
58
59
60

1
2
3
4
5
6
7
8
9
10
11
12
13
14
15
16
17
18
19
20
21
22
23
24
25
26
27
28
29
30
31
32
33
34
35
36
37
38
39
40
41
42
43
44
45
46
47
48
49
50
51
52
53
54
55
56
57
58
59
60

between neighboring BSs is less than the period of CP. For instance, the distance of two BSs should be no more than 1.41 km, corresponding to 4.69 μ s CP length in the case of 20 MHz LTE. From the technical perspective, however, this interference can be turned into useful signals according to the CoMP technology.

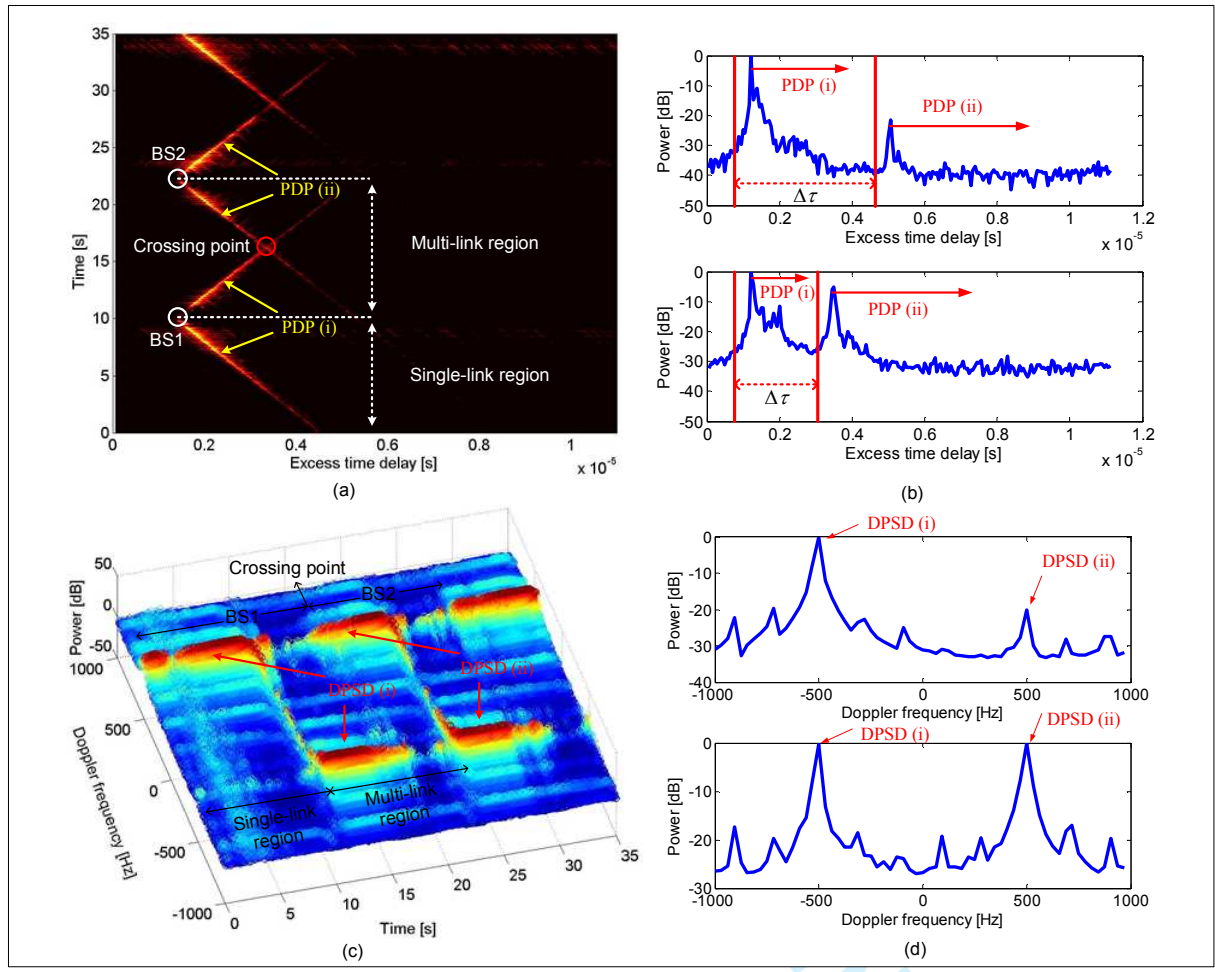


Figure 4. Results of the cell combination measurement in the RC scenario. (a) Time-variant PDP. (b) Two snapshots of the PDP in the multi-link region. The top one is captured when the train is close to BS1, whereas the bottom one is recorded when the train goes away from BS1. (c) Time-variant DPDS. (d) Two snapshots of the DPDS in the multi-link region. The top one is acquired when the train goes away from BS1, whereas the bottom one is obtained when the train is close to the crossing point.

Mobile Relay Measurement Results

Based on the measurement data in the single-link region, we highlight the RC measurement results, concentrating on path loss (PL) and root mean square (RMS) delay spread (DS), as seen in Fig. 5. For comparison, we also show the DC measurement results. Fig. 5(a) illustrates the ensemble PL results in all cells and PL models for the DC and RC cases. The PL in the DC scenario is found to be 20-30 dB higher than that

in the RC scenario. This value corresponds to the penetration loss of train car. On the other hand, the resulting PL exponents in the DC and RC scenarios are 3.16 and 3.76, respectively, which are all much higher than that in the free space propagation scenario. For the DC case it is understandable that the outdoor to indoor propagation condition has an impact on the PL exponent, however, for the RC case the main reason which has been explained in [6] [8] is that the train carriage roof would act as a ground plane and thus affect the antenna radiation pattern by causing a null in a certain incidence angle area of the radiation pattern. Fig. 5(b) depicts the CDFs of the RMS DS results. Since the in-train propagation environment causes the additional scattering and reflecting components, the RMS DS for the DC case is obviously higher than that for the RC case.

According to these results, we conclude that the mobile relay can not only enhance the coverage but also avoid the impact of the in-train environment. However, the problem of using mobile relay is that the received power would attenuate faster due to the distorted antenna radiation pattern caused by the train carriage roof.

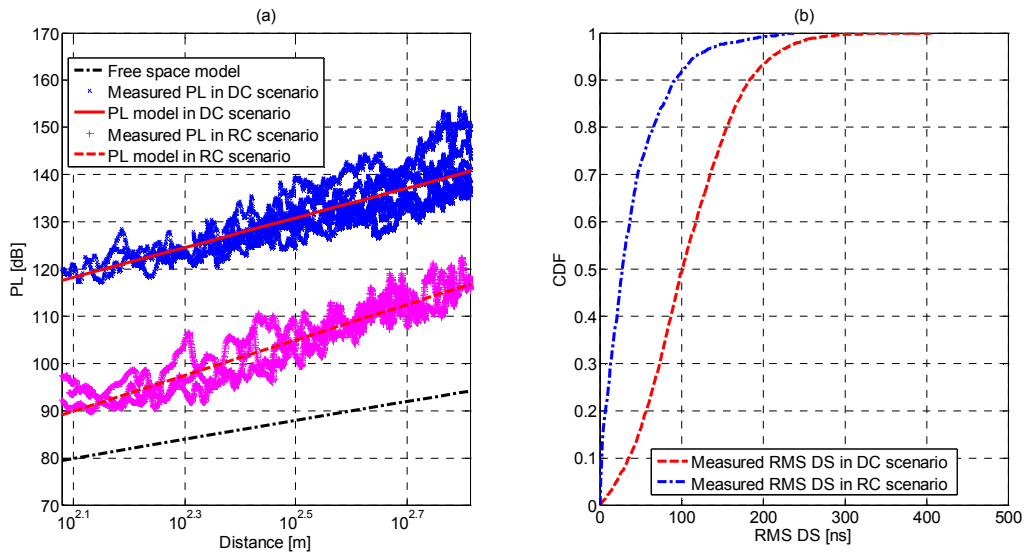


Figure 5. Comparison of the measurement results in the DC and RC scenarios.

MIMO and CoMP Measurement Results

For MIMO and CoMP channel characterization, we mainly focus on the single-link spatial correlation (SSC), single-link channel capacity (CC), and multi-link spatial correlation (MSC). The MSC exists due to the environment similarity arising from common scatterers contributing to different links [15]. We denote the measured CIR matrix in the single-link region as H_{ij}^S and the CIR matrices extracted from BS1 and BS2 in the multi-link region as $H_{ij}^{M,1}$ and $H_{ij}^{M,2}$, where i and j are the indices of the antenna elements at the

transmitter and the receiver, respectively. Based on the measurement data in the single-link region, the SSC between two sub-channels, e. g., H_{11}^S and H_{22}^S , are derived. Similarly, according to the effective measurement data (setting the threshold of $\Delta\tau$ as $1\ \mu\text{s}$) in the multi-link region, the MSC between $H_{11}^{M,1}$ and $H_{11}^{M,2}$ is estimated. Fig. 6 illustrates the results of SSC and CC in the RC scenario, and MSC in the DC and RC scenarios. The capacity for the independent and identically distributed (i.i.d.) complex Gaussian channel with zero mean and unit variance is also included. It is observed that almost 65% of SSC values are less than 0.8, and the corresponding CC approximates 10 bits/s/Hz in the case of 20 dB SNR. For the MSC, the results are optimistic in both DC and MRC scenarios where the majority of the correlation coefficient values are below 0.8. Moreover, since rich scatterers in the in-train environment lead to a low degree of environment similarity, the DC case has the lower MSC than the RC case.

From the above observations, we can infer that the cross polarized antenna configuration at the BS side and the large antenna spacing at the train side are beneficial to improve the MIMO performance in the LOS-dominant HSR scenario. In addition, CoMP will have a good performance in terms of micro-diversity due to the small MSC.

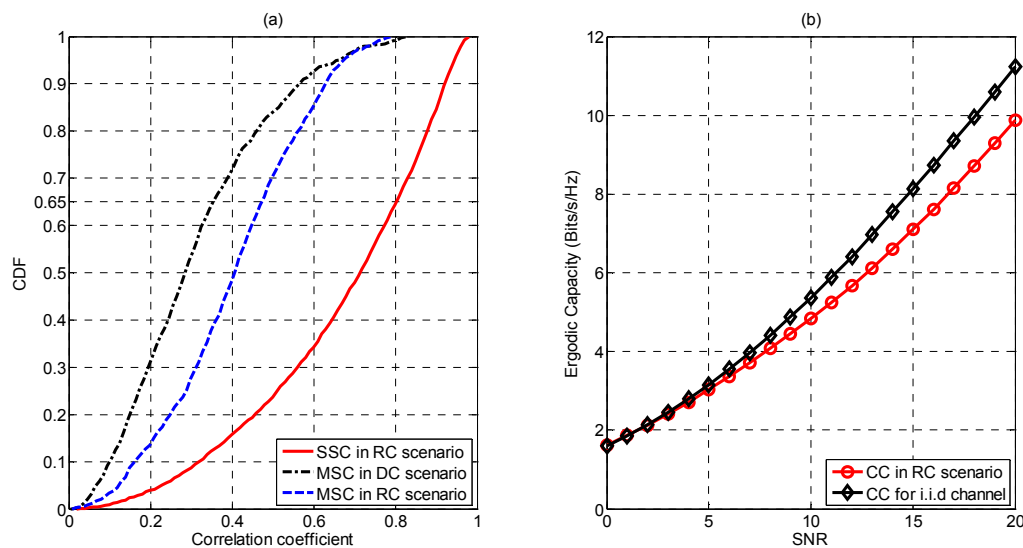


Figure 6. Results of the MIMO and CoMP measurements in the DC and RC scenarios.

Conclusion

In this article, we discuss the channel sounding issues for HSR communication systems. After

summarizing the requirements, challenges and recent advances in HSR channel measurements, we describe a novel LTE-based channel sounding scheme. Further, we show typical results from LTE-based measurement campaigns, concentrating on the evaluation of cell combination and mobile relay effects and the analysis of MIMO and CoMP performances. These field test results confirm the viability of the proposed scheme and provide useful information for the optimization of current HSR LTE systems and the design of future HSR communication systems.

Acknowledgement

The authors would like to thank Huisheng Wang and Yuzheng Zhang from China Academy of Railway Sciences for their help to perform the channel measurements, and Long Sun from Huawei for the useful discussion of LTE railway network structure and configuration. The research was supported in part by the NSFC project under grant No. 61371070, No. 61471030, and Beijing Natural Science Foundation (4142041).

References

- [1] B. Ai, X. Cheng, T. Kürner, Z. D. Zhong, K. Guan, R. S. He, L. Xiong, D. W. Matolak, D. G. Michelson, and C. B. Rodriguez, "Challenges toward wireless communications for high-speed railway," *IEEE Tran. Intell. Transp.*, vol. 15, no. 5, Oct. 2014, pp. 2143-2158.
- [2] Li Yan, Xuming Fang, and Yuguang Fang, "Control and data signaling decoupled architecture for railway wireless networks," *IEEE Wireless Commun.*, vol. 22, no. 1, Feb. 2015, pp. 103-111.
- [3] [Online]. Available: <http://www.huawei.com/za/static/HW-371906.pdf>
- [4] D. Soldani and S. Dixit, "Wireless relays for broadband access," *IEEE Commun. Mag.*, vol. 46, no. 3, Mar. 2008, pp. 58-66.
- [5] L. Zhu, F. Richard Yu, H. Wang, T. Tang, and B. Ning, "Design and performance enhancements in communication-based train control (CBTC) systems with coordinated multi-point transmission and reception (CoMP)," *IEEE Tran. Intell. Transp.*, vol. 15, no. 3, Jun. 2014, pp. 1258-1272.
- [6] P. Kyösti, "WINNER II channel models part II radio channel measurement and analysis results," 2007.
- [7] R. Parviainen, P. Kyösti, and Y. Hsieh, "Results of high speed train channel measurements," European Cooperation in the Field of Scientific and Technical Research, Tech. Rep., 2008.
- [8] L. Liu, C. Tao, J. H. Qiu, H. J. Chen, L. Yu, W. H. Dong, and Y. Yuan, "Position-based modeling for wireless channel on high-speed railway under a viaduct at 2.35 GHz," *IEEE J. Sel. Areas Commun.*, vol. 30, no. 4, May 2012, pp. 834-845.
- [9] R. S. He, Z. D. Zhong, B. Ai, and J. Ding, "An empirical path loss model and fading analysis for high-speed railway viaduct scenarios," *IEEE Antennas Wireless Propag. Lett.*, vol. 10, Aug. 2011, pp. 808-812.
- [10] J. H. Qiu, C. Tao, L. Liu, and Z. H. Tan, "Broadband channel measurement for the high-speed railway based on WCDMA," In *Proc. IEEE 75th Vehicular Technology Conf. (VTC Spring)*, Yokohama, Japan, May 2012, pp. 1-5.
- [11] S. Salous, Radio Propagation Measurement and Channel Modelling, John Wiley and Sons Ltd., Wiley, 2013.

- 1
2
3 [12] [Online]. Available: http://www.channelsounder.de/csprinciple_site2.html
4 [13] J. S. Jiang, M. F. Demirkol, and M. A. Ingram, "Measured capacities at 5.8 GHz of indoor MIMO systems with
5 MIMO interference," In *Proc. IEEE 58th Vehicular Technology Conf. (VTC Fall)*, Orlando, USA, Oct. 2003, pp.
6 388-393.
7
8 [14] T. Zhou, C. Tao, L. Liu, and Z. H. Tan, "A study on a LTE-based channel sounding scheme for high-speed railway
9 scenarios," In *Proc. IEEE 78th Vehicular Technology Conf. (VTC Fall)*, Las Vegas, USA, Sept. 2013, pp.1-5.
10
11 [15] X. Cheng, C.-X. Wang, H. Wang, X. Gao, X.-H. You, D. Yuan, B. Ai, Q. Huo, L. Song, and B. Jiao, "Cooperative
12 MIMO channel modeling and multi-link spatial correlation properties," *IEEE J. Sel. Areas Commun.*, vol. 30, no. 2,
13 Feb. 2012, pp. 388-396.
14
15
16
17
18
19
20
21
22
23
24
25
26
27
28
29
30
31
32
33
34
35
36
37
38
39
40
41
42
43
44
45
46
47
48
49
50
51
52
53
54
55
56
57
58
59
60

For Review Only